Photoluminescence decay time and electroluminescence of *p*-Si/*β*-$FeSi_2$ particles/*n*-Si and *p*-Si/*β*-$FeSi_2$ film/*n*-Si double-heterostructures light-emitting diodes grown by molecular-beam epitaxy

T. Suemasu, Y. Ugajin, S. Murase, T. Sunohara, and M. Suzuno
Institute of Applied Physics, University of Tsukuba, 1-1-1 Tennohdai, Tsukuba, Ibaraki 305-8573, Japan

(Received 4 April 2007; accepted 7 May 2007; published online 25 June 2007)

We have epitaxially grown Si/*β*-$FeSi_2$/Si (SFS) structures with *β*-$FeSi_2$ particles on Si(001), and SFS structures with *β*-$FeSi_2$ continuous films on both Si(001) and Si(111) substrates by molecular-beam epitaxy. All the samples exhibited the same photoluminescence (PL) peak wavelength of approximately 1.54 μm at low temperatures. However, the PL decay times for the 1.54 μm emission were different, showing that the luminescence originated from different sources. The decay curves of the SFS structures with *β*-$FeSi_2$ continuous films were fitted assuming a two-component model, with a short decay time ($\tau \sim 10$ ns) and a long decay time ($\tau \sim 100$ ns), regardless of substrate surface orientation. The short decay time was comparable to that obtained in the SFS structure with *β*-$FeSi_2$ particles. The short decay time was due to carrier recombination in *β*-$FeSi_2$, whereas the long decay time was probably due to a defect-related *D*1 line in Si. We obtained 1.6 μm electroluminescence (EL) at a low current density of 2 A/cm^2 up to around room temperature. The temperature dependence of the EL peak energy of the SFS diodes with *β*-$FeSi_2$ particles can be fitted well by the semiempirical Varshni's law. However, EL peak positions of the SFS diodes with the *β*-$FeSi_2$ films showed anomalous temperature dependence; they shifted to a higher energy with increasing temperature, and then decreased. These results indicate that the EL emission originated from several transitions.
© *2007 American Institute of Physics*. [DOI: 10.1063/1.2749200]

I. INTRODUCTION

Semiconducting iron disilicide (*β*-$FeSi_2$) has been attracting significant recent interest as a Si-based light emitter, ever since electroluminescence (EL) was demonstrated from *β*-$FeSi_2$ precipitates embedded in Si *pn* diodes on Si(001) substrates.[1] The emission wavelength of 1.6 μm at room temperature (RT) corresponds to a low loss window of the Si/SiO_2 photonic wire waveguide.[2,3] We therefore believe that *β*-$FeSi_2$ is a very promising material for a light emitter for optical interconnects in Si integrated circuits. There have been several reports to date on the EL of *β*-$FeSi_2$ at RT.[4–10] Most of them are for light-emitting diodes (LEDs) made of Si/*β*-$FeSi_2$/Si (SFS) structures with *β*-$FeSi_2$ particles on Si(001), formed by ion beam synthesis (IBS) and reactive deposition epitaxy (RDE). In the case of RDE, a *β*-$FeSi_2$ epitaxial film on Si(001) exhibits a strong tendency to agglomerate at high temperatures.[11] In the case of IBS, lower doses of Fe are implanted to form *β*-$FeSi_2$ precipitates to decrease defect densities.[12] Further work has been done to enhance the luminescence of *β*-$FeSi_2$.[13] In an effort to make an efficient LED, it is necessary to embed a continuous *β*-$FeSi_2$ film rather than particles in Si. Very recently, SFS double-heterostructure (DH) LEDs on Si(111), that is, SFS LEDs with *β*-$FeSi_2$ continuous film active region, have been realized by molecular-beam epitaxy (MBE) and by sputtering,[6,7,14,15] and 1.6 μm EL was achieved at RT. We have also started the formation of SFS DH LEDs on Si(001).[16,17] The reported luminescence is considered to originate from recombination in the *β*-$FeSi_2$. However, it has also been suggested that the luminescence may be related to defects in the Si. The characteristic *D*1 line, in particular, corresponds to the 1.54 μm emission line for *β*-$FeSi_2$ at low temperatures.[18–21] Thus, a simple steady-state photoluminescence (PL) measurement alone cannot distinguish the luminescence of *β*-$FeSi_2$ from a *D*1 line. Time-resolved PL measurement, as compared to steady-state PL measurement, is considered to be a very powerful method for investigating the intrinsic optical properties of *β*-$FeSi_2$. *β*-$FeSi_2$ has been fabricated by various growth techniques such as RDE, MBE, IBS, pulsed laser deposition, metal-organic chemical vapor deposition, etc. However, there have only been a very limited number of reports discussing the decay time of the 1.54 μm PL line of *β*-$FeSi_2$.[14,22–26] We should also note that there have been no reports comparing the luminescence of SFS DH to that of SFS with *β*-$FeSi_2$ particles in detail. Thus, it is meaningful to measure PL decay times and to investigate the difference in luminescence of *β*-$FeSi_2$ between SFS DH and SFS with *β*-$FeSi_2$ particles, formed in the same growth chamber. We have been developing an epitaxial growth technique for *β*-$FeSi_2$ on Si substrates and SFS structures. Our group is the only one so far that has realized 1.6 μm EL at RT in both SFS LEDs with *β*-$FeSi_2$ precipitates and SFS DH LEDs.[2,4,7]

In this study, we have measured the PL decay times of SFS DH on both Si(001) and Si(111) substrates as well as

 © 2007 American Institute of Physics

Downloaded 06 Jan 2010 to 130.158.56.186. Redistribution subject to AIP license or copyright; see http://jap.aip.org/jap/copyright.jsp

TABLE I. Sample preparation: growth temperature and thickness of RDE- and MBE-grown β-$FeSi_2$ layers. The thickness of the Si overlayer is listed in parentheses. Annealing conditions are also specified.

Sample	RDE/MBE	Si overlayer	Post annealing
A	470 °C (10 nm)	500 °C (400 nm)	900 °C/14 h
B	470 °C (8 nm)	500 °C (400 nm)	no
C	650 °C (20 nm)/750 °C (250 nm)	500 °C (900 nm)	900 °C/14 h

those of SFS with β-$FeSi_2$ particles. The origin of 1.54 μm PL and the difference in EL between SFS LEDs with β-$FeSi_2$ particles and SFS DH LEDs are discussed.

II. EXPERIMENTAL METHOD

An ion-pumped MBE system equipped with electron gun evaporation sources for 10N-Si and 5N-Fe was used in this investigation. SFS structures with β-$FeSi_2$ particles active region were fabricated on Si(001) as follows. First, 10-nm-thick [100]-oriented β-$FeSi_2$ epilayers were grown on *n*-Si(001) substrates by RDE at 470 °C.[27,28] The sample was then annealed *in-situ* at 850 °C for 1 h to improve the crystal quality of the β-$FeSi_2$. The β-$FeSi_2$ film agglomerates into islands during this process. Consequently, a 400-nm-thick undoped *p*-Si layer was grown by MBE at 500 °C. Samples were finally annealed at 900 °C for 14 h in an Ar atmosphere, resulting in β-$FeSi_2$ particles embedded in the Si matrix. Agglomeration of the β-$FeSi_2$ is considered to occur so that the interface energy due to the lattice mismatch minimizes by decreasing the contact area between the two materials. This sample was denoted as sample *A*. Fabrication of an SFS DH on Si(001) was carried out as follows. [100]-oriented 8-nm-thick β-$FeSi_2$ films were grown on *n*-Si(001) substrates by RDE at 470 °C. This thickness of 8 nm was an optimum value as determined in our previous study.[15] Next, a 400-nm-thick undoped *p*-Si layer was grown by MBE at 500 °C. High-temperature annealing was not performed for this sample, because the β-$FeSi_2$ layer embedded in the Si agglomerates into β-$FeSi_2$ particles by high-temperature annealing, and the PL intensity decreases.[16] This sample was denoted as sample *B*. For an SFS DH on Si(111), a 20-nm-thick β-$FeSi_2$ epilayer was grown by RDE at 650 °C, and this film was used as a template to control the crystal orientation of a β-$FeSi_2$ overlayer. Si and Fe were then coevaporated on the β-$FeSi_2$ template at 750 °C by MBE to form 270-nm-thick β-$FeSi_2$ in total, followed by a 900-nm-thick undoped *p*-Si layer by MBE. To improve the crystal quality, 900 °C annealing was performed at 14 h in Ar.[13] For EL measurements, a boron-doped p^+-Si layer with a hole concentration of 2×10^{18} cm^{-3} was grown at 700 °C on top of samples *A* and *C* by simultaneous evaporation of Si and HBO_2. Details of the growth procedure were described in our previous report.[29] Samples were prepared as summarized in Table I.

The crystalline quality of the grown films was characterized by x-ray diffraction (XRD). Steady-state PL measurements were performed by the standard lock-in technique using a He-Cd laser (442 nm) and a liquid-nitrogen-cooled InP/InGaAs photomultiplier (PMT) (R5509–72, Hamamatsu Photonics, Japan). Time-resolved PL was measured using a time-correlated single-photon counting setup. The R5509–72 PMT served as a detector. The excitation wavelength, pulse width, and repetition rate were 532 nm, 0.6 ns, and 18 kHz, respectively. For EL measurements, a 1.5-mm^2 mesa structure was formed by wet chemical etching. An Al finger-type ohmic contact was formed on the *p*-Si layer and sintered at 450 °C for 20 min. The back surface contact was formed using AuSb.

III. RESULTS AND DISCUSSION

A. Growth of SFS structures

Figures 1(a)–1(c) show θ-2θ XRD patterns of samples *A*, *B*, and *C*, respectively. As shown in Fig. 1(a), no peaks other than those from [100]-oriented β-$FeSi_2$ can be observed. This orientation of β-$FeSi_2$ to the Si(001) surface agrees with the epitaxial face relationship between the two materials.[27] The 900 °C annealing enhances the diffraction intensity in sample *A*. The same epitaxial orientation was observed in sample *B*, as shown in Fig. 1(b) although the diffraction intensities are small. On the other hand, [110]- or [101]-oriented β-$FeSi_2$ matches the epitaxial face relationship of β-$FeSi_2$ on Si(111).[30] Figure 1(c), therefore, indicates that the β-$FeSi_2$ was epitaxially grown on Si(111). With regard to the electrical properties of undoped β-$FeSi_2$ films grown by MBE using high-purity 5N-Fe, the β-$FeSi_2$ films show *p*-type conductivity with a hole concentration of approximately 5×10^{17}–10^{18} cm^{-3} at RT. The hole concentration decreases down to the order of 10^{16} cm^{-3} at 100 K. The

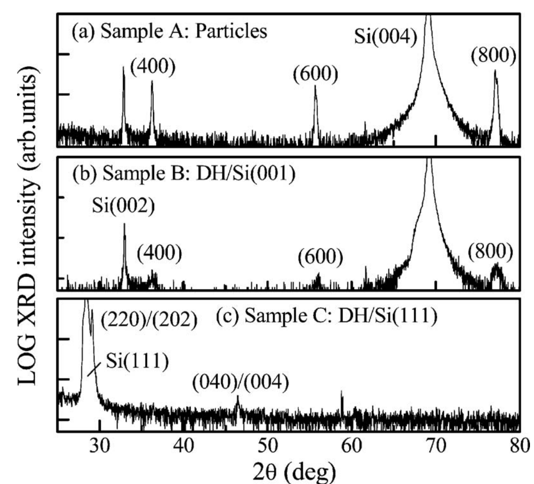

FIG. 1. θ-2θ XRD patterns of samples *A*, *B*, and *C*.

Downloaded 06 Jan 2010 to 130.158.56.186. Redistribution subject to AIP license or copyright; see http://jap.aip.org/jap/copyright.jsp

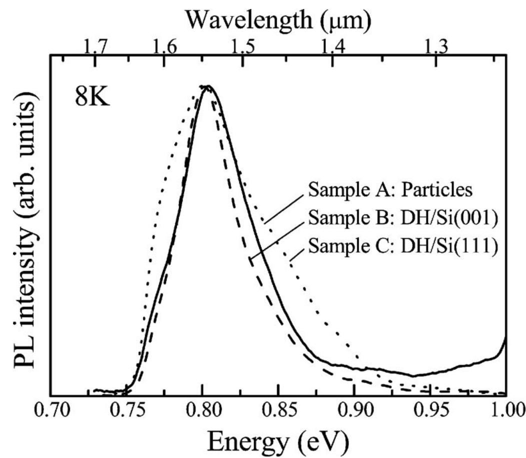

FIG. 2. Normalized PL spectra measured at 8 K for samples *A*, *B*, and *C*.

electrical properties are not the main subject of this study, and the details of electrical properties measurements will be reported elsewhere.

B. Photoluminescence

Figure 2 shows normalized PL spectra of samples *A*, *B*, and *C* measured at 8 K. Distinct PL was obtained even in sample *B*, which was not annealed at a high temperature. All the samples have a peak wavelength of approximately 1.54 μm, although the PL spectrum of sample *C*, SFS DH on Si(111), was broader than those for the other two samples. Stressed Si has been reported to introduce dislocations in the Si as well as exhibit characteristic *D*-line emissions.[18–21] The origin of this broad PL spectrum is therefore thought to be the dislocations.

For detailed investigation of the 1.54 μm PL, time-resolved PL was performed at around 80 K. The wavelength resolution was limited by the slit opening of the monochromator, and was approximately 15 nm. The time resolution of the system was approximately 1 ns. The PL decay curves of the 1.54 μm PL from samples *A*, *B*, and *C* are shown in Fig. 3. The decay curve obtained from sample *A*, SFS with β-$FeSi_2$ particles, could be explained well, as shown by the solid white line in Fig. 3, by one exponential decay curve with a decay time of 15 ns. The decay time of this sample was previously reported,[26] and was used as a reference in this work. In contrast, the decay curves obtained from samples *B* and *C*, SFS DH, cannot be fitted to one exponential decay curve, but can be fitted using Eq. (1), which is based on the assumption that it is composed of the sum of two exponentials as

$$I(t) = I_1 \exp\left(-\frac{t}{\tau_1}\right) + I_2 \exp\left(-\frac{t}{\tau_2}\right). \quad (1)$$

Here, I_1 and I_2 are the PL intensities of the components with decay times of τ_1 and τ_2, respectively. When τ_1 and τ_2 are 15 and 97 ns, respectively, the experimental curve of sample *B* is reproduced well. The experimental curve of sample *C* is fitted well when τ_1 and τ_2 are 15 and 104 ns, respectively. We cannot rule out other components with different decay times, but it can at least be stated that the two components are dominant.

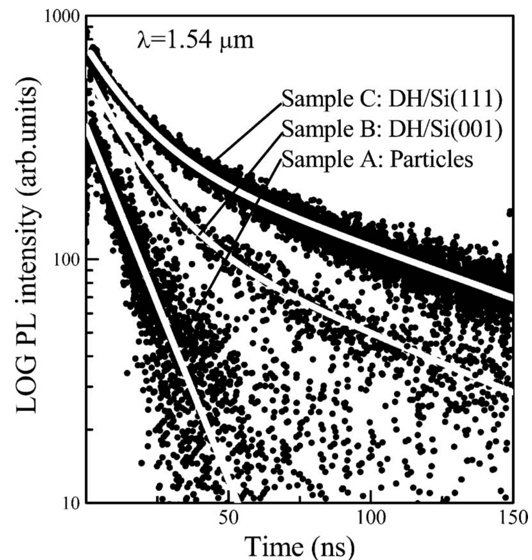

FIG. 3. Time-resolved PL decay curves of the 1.54 μm emission for samples *A*, *B*, and *C*, measured at 80, 70, and 80 K, respectively. White lines are fits using a two-component model for samples *B* and *C*.

In order to investigate the temperature dependence of decay times, time-resolved PL measurements were performed from 8 to around 150 K. PL decay curves for samples *B* and *C* can be described well by two discrete decay times over the entire temperature range. Figure 3 shows a typical example of PL decay curves obtained from sample *C*. In contrast, PL decay curves of sample *A* were fitted almost to one exponential decay component as in the case of the PL decay curve obtained at 80 K (see Fig. 4).

Figure 5 shows the obtained PL decay times versus temperature plots. As seen in the figure, the PL emission of samples *B* and *C* exhibited two different decay times over a wide temperature range. The short decay times were of the same order as those obtained from sample *A*, and they are less dependent on the temperature. The origin of these short

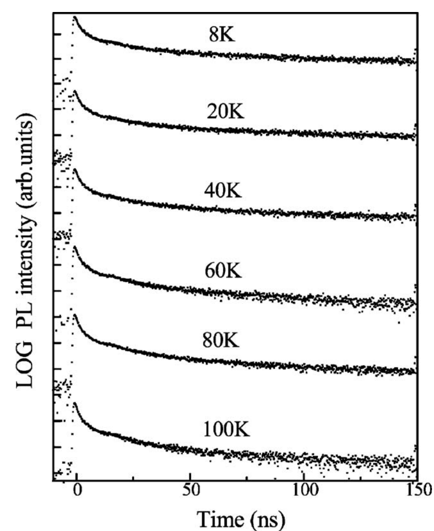

FIG. 4. Temperature dependence of PL decay curves of the 1.54 μm emission from sample *B*.

Downloaded 06 Jan 2010 to 130.158.56.186. Redistribution subject to AIP license or copyright; see http://jap.aip.org/jap/copyright.jsp

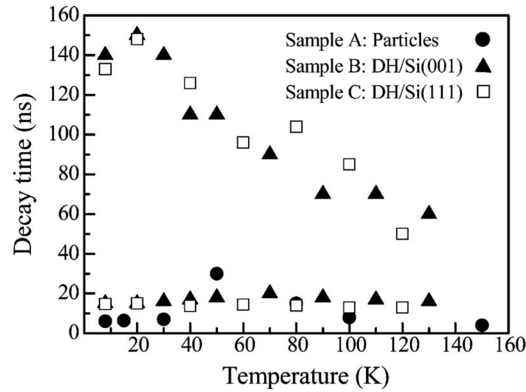

FIG. 5. PL decay time versus temperature obtained from the decay curves of samples *A*, *B*, and *C*.

decay times is considered to be recombination in β-$FeSi_2$. On the other hand, the long decay time obtained for samples *B* and *C* is considered to be due to the *D*1 luminescence. This is because the *D*1 line is another origin of the 1.54 μm PL. In addition, the long decay time obtained was comparable to the reported *D*1 decay times.[31] The decay time was observed to decrease with increasing temperature, indicating that the nonradiative recombination rate increases. On the basis of the above discussion, the origin of the short and long decay times in samples *B* and *C* is thought to be recombination in β-$FeSi_2$ and the defects in Si, respectively, regardless of the substrate surface orientation.

Figure 6 shows the temperature dependence of the PL intensity ratio of the fast I_{fast} to slow I_{slow} component. The fast and slow components correspond to the luminescence of β-$FeSi_2$ and *D*1 line, respectively. The ratio increases with increasing temperature. This increase was thought to be due to the fact that the *D*1 line was more rapidly quenched. This finding suggests that luminescence from β-$FeSi_2$ dominates at higher temperatures even in SFS DH. We should also note that the ratio of the luminescence of β-$FeSi_2$ is larger for sample *B* than for sample *C*. We speculate that this difference can be attributed to the difference in lattice mismatch between Si and β-$FeSi_2$, which is approximately 2.0% for [100]-oriented β-$FeSi_2$ on Si(001) in sample *B*, and approximately 5.5% for [110]- or [101]-oriented β-$FeSi_2$ on Si(111) in sample *C*.[27,30] The large lattice mismatch might induce lots of defects in Si, giving rise to luminescence with the *D*1 line being dominant. Very recently, Nakamura *et al.* reported

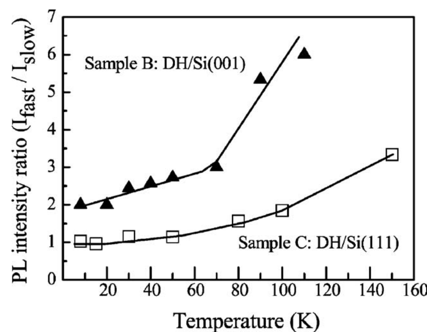

FIG. 6. Temperature dependence of the PL intensity ratio of the fast I_{fast} to slow I_{slow} component for samples *B* and *C*.

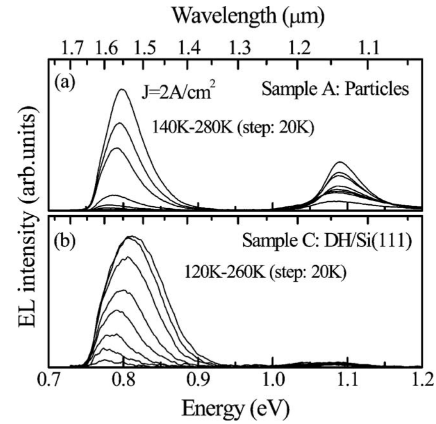

FIG. 7. Temperature dependence of EL spectra for samples *A* and *C*. The current density *J* was 2 A/cm^2.

the formation of β-$FeSi_2$ nanoislands with a height of approximately 2–5 nm epitaxially grown on Si(111) surfaces. These kinds of nanoislands, which had no misfit dislocations near the β-$FeSi_2$/Si interface, may suffer less influence from the large lattice mismatch between β-$FeSi_2$ and Si.[32,33]

C. Electroluminescence

The temperature dependence of the EL spectra was measured for samples *A* and *C* except sample *B*, as shown in Figs. 7(a) and 7(b), respectively. The current density *J* was kept constant at 2 A/cm^2. We have also realized the 1.6 μm EL at RT for sample *B*, SFS DH LED on Si(001).[17] However, electron injection is difficult at low temperatures in sample *B* due to a low hole concentration (10^{16} cm^{-3}) in its *p*-Si capping layer. That is why we excluded sample *B* for this measurement. In order to form a p^+-Si layer using HBO_2, at least 700 °C is necessary;[29] however, the 8-nm-thick β-$FeSi_2$ in sample *B* agglomerates into β-$FeSi_2$ particles at this temperature. We have not yet succeeded in forming p^+-Si layers in sample *B* while preventing the agglomeration of β-$FeSi_2$ layers. Thus, in this work, we have compared the temperature dependence of EL between samples *A* and *C*.

The EL spectra of sample *C* are broader than those of sample *A* as in the case of the PL spectra shown in Fig. 2, indicating that defect-related luminescence in Si exists in sample *C*. The emission around 1.10 eV in sample *A* is attributed to radiative recombination in Si with the assistance of transverse optical (TO) phonons (58 meV).[34] The EL peak energy of the two samples is plotted as a function of temperature in Fig. 8. The experimental dependence of the EL peak energy of sample *A* can be fitted well to the broken line by applying the semiempirical Varshni's law with parameters of $\alpha=2.5\times10^{-4}$ eV/K and $\beta=230$ K.[35] This result indicates that this emission originated in the band-to-band recombination of carriers in β-$FeSi_2$ On the other hand, the peak energy of sample *C* increased up to around 70 K, and then decreased. This anomalous temperature dependence was considered to be due to the fact that the broad luminescence is composed of several luminescence peaks, and their temperature dependence is different, giving rise to such anoma-

Downloaded 06 Jan 2010 to 130.158.56.186. Redistribution subject to AIP license or copyright; see http://jap.aip.org/jap/copyright.jsp

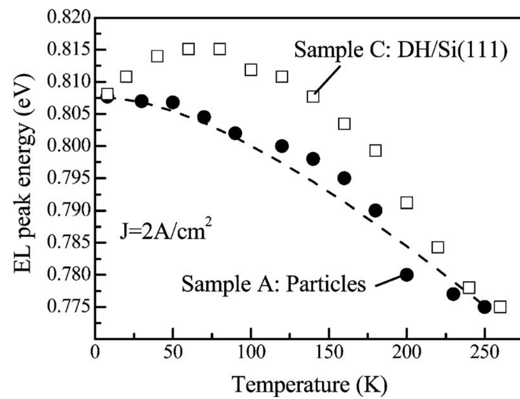

FIG. 8. Temperature dependence of EL peak energy for samples A and C. The current density J was 2 A/cm^2. The broken line is the fit obtained by applying the semiempirical Varshni law with parameters of α=2.5 $\times 10^{-4}$ eV/K and β=230 K.

lous dependence. This interpretation is consistent with the fact that the 1.54 μm PL in sample C was composed of at least two components.

Figure 9 shows thermal quenching of the normalized integrated EL intensity of samples A and C when the J value was 2 A/cm^2. In the model of the nonradiative recombination, the emission intensity for the nonradiative recombination can be described as:

$$I(T) = I_0[1 + C \exp(-E/k_B T)]. \quad (2)$$

Here, E is an activation energy for nonradiative recombination, and I_0 and C are temperature-independent coefficients, k_B is the Boltzmann's constant and T is the absolute temperature.[36] The activation energies of samples A and C are 0.18 and 0.13 eV, respectively, above 160 K. The value of 0.18 eV in sample A is close to the reported conduction band discontinuity at β-$FeSi_2$/Si,[37] and also to that obtained in PL measurements,[22,38] showing the thermal excitation of carriers in β-$FeSi_2$ over the heterostructure barrier. On the other hand, the smaller value of 0.13 eV indicates the existence of other routes to nonradiative recombination pathways. On the basis of the above discussion, we conclude that other luminescence such as the $D1$ line is considered to contribute to the EL from SFS DH LEDs.

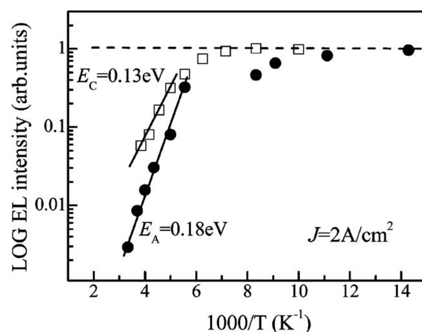

FIG. 9. Normalized integrated EL intensity versus inverse temperature for samples A and C at J=2 A/cm^2. Activation energies of 0.18 eV (E_A) and 0.13 eV (E_C) were obtained, respectively.

IV. SUMMARY

We have epitaxially grown SFS structures with β-$FeSi_2$ particles on Si(001), and SFS DH on both Si(001) and Si(111) substrates by MBE. All the samples exhibited the same PL peak wavelength of 1.54 μm at low temperatures. However, the PL decay time of 1.54 μm emission was different. The decay curves of the SFS DH structures were fitted well by assuming a two-component model, with a short decay time ($t \sim 10$ ns) and a long decay time ($t \sim 10$ ns), regardless of the substrate surface orientation. In contrast, a short decay time ($t \sim 10$ ns) was found to be dominant in the SFS structure with β-$FeSi_2$ particles. The short decay time was due to carrier recombination in β-$FeSi_2$, as in the case of the SFS structure with β-$FeSi_2$ particles. On the other hand, the long decay time was probably due to a defect-related $D1$ line in Si. The temperature dependence of the EL peak energy of SFS diodes with β-$FeSi_2$ particles can be fitted well using the semiempirical Varshni's law. On the other hand, the EL peak positions of SFS DH on Si(111) showed anomalous temperature dependence, indicating that the luminescence was composed of several emission peaks. These results indicate that other luminescence such as the $D1$ line was considered to contribute to the EL from the SFS DH LEDs.

ACKNOWLEDGMENTS

This work was supported in part by the Ministry of Education, Culture, Sports, Science and Technology of Japan (MEXT), and the Industrial Technology Research Grant Program from the New Energy and Industrial Technology Development Organization (NEDO) of Japan.

[1]D. Leong, M. Harry, K. J. Reeson, and K. P. Homewood, Nature (London) **387**, 686 (1997).
[2]T. Suemasu, Y. Negishi, K. Takakura, and F. Hasegawa, Jpn. J. Appl. Phys., Part 2 **39**, L1013 (2000).
[3]M. A. Lourenco, T. M. Butler, A. K. Kewell, R. M. Gwilliam, K. J. Kirkby, and K. P. Homewood, Jpn. J. Appl. Phys., Part 1 **40**, 4041 (2001).
[4]T. Suemasu, Y. Negishi, K. Takakura, F. Hasegawa, and T. Chikyow, Appl. Phys. Lett. **79**, 1804 (2001).
[5]L. Martinelli, E. Grilli, M. Guzzi, and M. G. Grimaldi, Appl. Phys. Lett. **83**, 794 (2003).
[6]S. Chu, T. Hirohada, H. Kan, and T. Hiruma, Jpn. J. Appl. Phys., Part 2 **43**, L154 (2004).
[7]M. Takauji, C. Li, T. Suemasu, and F. Hasegawa, Jpn. J. Appl. Phys., Part 1 **44**, 2483 (2005).
[8]T. Sunohara, C. Li, Y. Ozawa, T. Suemasu, and F. Hasegawa, Jpn. J. Appl. Phys., Part 1 **44**, 3951 (2005).
[9]Cheng Li, T. Suemasu, and F. Hasegawa, J. Appl. Phys. **97**, 043529 (2005).
[10]Cheng Li, T. Suemasu, and F. Hasegawa,, J. Lumin. **118**, 330 (2006).
[11]T. Suemasu, M. Tanaka, T. Fujii, S. Hashimoto, Y. Kumagai, and F. Hasegawa, Jpn. J. Appl. Phys., Part 2 **36**, L1225 (1997).
[12]T. D. Hunt, B. J. Sealy, K. J. Reeson, R. M. Gwilliam, K. P. Homewood, R. J. Wilson, C. D. Meekison, and G. R. Booker, Nucl. Instrum. Methods Phys. Res. B **74**, 60 (1993).
[13]Y. Terai and Y. Maeda, Appl. Phys. Lett. **84**, 903 (2004).
[14]M. Takauji, C. Li, T. Suemasu, F. Hasegawa, and M. Ichida, J. Appl. Phys. **96**, 2561 (2004).
[15]Y. Ugajin, M. Takauji, and T. Suemasu, Thin Solid Films **508**, 376 (2006).
[16]T. Sunohara, K. Kobayashi, and T. Suemasu, Thin Solid Films **508**, 371 (2006).
[17]S. Murase, T. Sunohara, and T. Suemasu, J. Cryst. Growth **301–302**, 676 (2007).
[18]D. A. Drozdov, A. A. Patrin, and V. D. Tkachev, JETP Lett. **23**, 597 (1976).

Downloaded 06 Jan 2010 to 130.158.56.186. Redistribution subject to AIP license or copyright; see http://jap.aip.org/jap/copyright.jsp

[19]B. Suezawa, Y. Sasaki, and K. Sumio, Phys. Status Solidi A **79**, 173 (1983).
[20]R. Sauer, J. Weber, J. Stolz, E. Weber, K. Kusters, and H. Alexander, Appl. Phys. A: Solids Surf. **36**, 1 (1985).
[21]A. A. Shklyaev, Y. Nakamura, and M. Ichikawa, J. Appl. Phys. **101**, 033532 (2007).
[22]C. Spinella, S. Coffa, C. Bongiorno, S. Pannitteri, and M. G. Grimaldi, Appl. Phys. Lett. **76**, 173 (2000).
[23]B. Schuller, R. Carius, S. Lenk, and S. Mantl, Microelectron. Eng. **60**, 205 (2002).
[24]B. Schuller, R. Carius, and S. Mantl, J. Appl. Phys. **94**, 207 (2003).
[25]S. Chu, T. Hirohada, M. Kuwabara, H. Kan, and T. Hiruma, Jpn. J. Appl. Phys., Part 2 **43**, L127 (2004).
[26]T. Suemasu, M. Takauji, C. Li, Y. Ozawa, M. Ichida, and F. Hasegawa, Jpn. J. Appl. Phys., Part 2 **43**, L930 (2004).
[27]J. E. Mahan, K. M. Geib, G. Y. Robinson, R. G. Long, X. Yan, G. Bai, M. A. Nicolet, and M. Nathan, Appl. Phys. Lett. **56**, 2126 (1990).
[28]M. Tanaka, Y. Kumagai, T. Suemasu, and F. Hasegawa, Jpn. J. Appl. Phys., Part 1 **36**, 3620 (1997).
[29]Cheng Li, T. Ohtsuka, Y. Ozawa, T. Suemasu, and F. Hasegawa, J. Appl. Phys. **94**, 1518 (2003).
[30]J. E. Mahan, V. Le Thanh, J. Chevrier, I. Berbezier, J. Derrien, and R. G. Long, J. Appl. Phys. **74**, 1747 (1993).
[31]S. Fukatsu, Y. Mera, M. Inoue, K. Maeda, H. Akiyama, and H. Sakaki, Appl. Phys. Lett. **68**, 1889 (1996).
[32]Y. Nakamura, R. Suzuki, M. Umeno, S. P. Cho, N. Tanaka, and M. Ichikawa, Appl. Phys. Lett. **89**, 123104 (2006).
[33]Y. Nakamura, Y. Nagadomi, S. P. Cho, N. Tanaka, and M. Ichikawa, J. Appl. Phys. **100**, 044313 (2006).
[34]S. Fukatsu, N. Usami, and Y. Shiraki, Jpn. J. Appl. Phys., Part 1 **32**, 1502 (1993).
[35]Y. P. Varshni, Physica (Amsterdam) **34**, 149 (1967).
[36]J. I. Pankove, *Optical Processes in Semiconductors* (Dover, New York, 1971).
[37]L. Martinelli, E. Grilli, D. B. Migas Leo. Miglio, F. Marabelli, C. Soci, M. Geddo, M. G. Grimaldi, and C. Spinella, Phys. Rev. B **66**, 085320 (2002).
[38]T. Suemasu, Y. Iikura, K. Takakura, and F. Hasegawa, J. Lumin. **87–89**, 528 (2000).

Downloaded 06 Jan 2010 to 130.158.56.186. Redistribution subject to AIP license or copyright; see http://jap.aip.org/jap/copyright.jsp